Phytochemistry 220 (2024) 114031

Contents lists available at ScienceDirect

Phytochemistry

journal homepage: www.elsevier.com/locate/phytochem

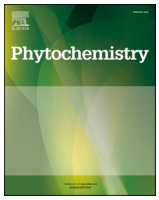

Undescribed sesquiterpenoids with NO production inhibitory activity from oleo-gum resin of *Commiphora myrrha*

Bingyang Zhang [a,1], Wenhua Chao [a,1], Weiyun Di [a,1], Shijie Cao [b,**], Paul Owusu Donkor [c], Lining Wang [a], Feng Qiu [a,b,*]

[a] Tianjin Key Laboratory of Therapeutic Substance of Traditional Chinese Medicine, School of Chinese Materia Medica, Tianjin University of Traditional Chinese Medicine, Tianjin, 301617, China
[b] State Key Laboratory of Component-based Chinese Medicine, Tianjin University of Traditional Chinese Medicine, Tianjin, 301617, China
[c] School of Pharmacy, University of Ghana, Accra, Ghana

ARTICLE INFO

Keywords:
Commiphora myrrha
Myrrh
Burseraceae
Sesquiterpenoids
NO production
Anti-inflammatory activity

ABSTRACT

Six undescribed cadinane sesquiterpenoids (**1**−**6**), two undescribed guaiane sesquiterpenoids (**7**−**8**), and an undescribed germacrane sesquiterpenoid (**9**) were isolated from the oleo-gum resin of *Commiphora myrrha*. Their structures were determined by the analysis of 1D/2D NMR and HRESIMS data, as well as quantum chemical ECD and NMR calculations. All the sesquiterpenoids were evaluated for their NO production inhibitory activity in LPS-stimulated RAW 264.7 mouse monocyte-macrophages. The results revealed that commiphone A (**1**) and commipholide D (**7**) exhibited significant inhibitory effect on NO generation with IC_{50} values of 18.6 ± 2.0 and 37.5 ± 1.5 μM, respectively. Furthermore, **1** and **7** dose-dependently inhibited the mRNA expression of inflammatory cytokines IL-1β, IL-6 and TNF-α induced by LPS in the RAW264.7 cells, indicating that **1** and **7** possess potent anti-inflammatory activity *in vitro*.

1. Introduction

Myrrh, originating from Arabia, is an oleo-gum resin exuded from wounded stem surfaces of *Commiphora* species. The genus *Commiphora* belongs to Burseraceae family and is made up of over 150 species distributed in subtropical and tropical regions, particularly Arabian Peninsula and northeastern Africa (Demissew et al., 1993). *Commiphora myrrha* (Nees) Engl., which is responsible for the production of myrrh, has been used for the treatment of inflammation, infections, burns, obesity, and gastrointestinal diseases in Arabia, Africa, India and China since time immemorial (Abdul-Ghani et al., 2009; Committee of the Chinese Pharmacopoeia, 2020). Previous phytochemical investigations on *Commiphora* species have revealed more than 300 structurally characterized components, and terpenoids especially the sesqui- and triterpenoids are the most abundant constituents (Abdul-Ghani et al., 2009; Shen et al., 2012). Meanwhile, a wide range of biological activities such as anti-inflammatory, anti-cancer, antioxidant, anti-microbial, neuroprotective, and anti-diabetic effects have been found in the extracts and chemical components of myrrh (Yu et al., 2020; Wang et al., 2022; Bao et al., 2021; Sun et al., 2020; Khalil et al., 2020; Al-Romaiyan et al., 2021). In an ongoing effort for the discovery of bioactive constituents from the resin of medicinal plants (Zhang et al., 2021; Zhang et al., 2022), six undescribed cadinane sesquiterpenoids (**1**−**6**), two undescribed guaiane sesquiterpenoids (**7**−**8**), and an undescribed germacrane sesquiterpenoid (**9**) were isolated from the oleo-gum resin of *C. myrrha* (Fig. 1). The NO production inhibitory activity of all the sesquiterpenoids was evaluated by testing NO production and the mRNA expression of several inflammatory factors induced by lipopolysaccharide (LPS) in RAW 264.7 macrophages. Detailed procedures and results of the isolation, structural elucidation, and NO production inhibitory activity of these compounds are reported herein.

* Corresponding author. Tianjin University of Traditional Chinese Medicine, 10 Poyanghu Road, West Area, Tuanbo New Town, Jinghai District, Tianjin, 301617, China.
** Corresponding author. Tianjin University of Traditional Chinese Medicine, 10 Poyanghu Road, West Area, Tuanbo New Town, Jinghai District, Tianjin, 301617, China.
E-mail addresses: shijiecao0421@hotmail.com (S. Cao), fengqiu20070118@163.com (F. Qiu).
[1] These authors made equal contributions to this work.

https://doi.org/10.1016/j.phytochem.2024.114031
Received 8 November 2023; Received in revised form 12 February 2024; Accepted 15 February 2024
Available online 16 February 2024

2. Results and discussion

Commiphone A (**1**) was obtained as pale yellow needles (MeOH), and its molecular formula was determined as $C_{15}H_{16}O_3$ by the HRESIMS positive ion at *m/z* 245.1167 $[M + H]^+$ (calcd for $C_{15}H_{17}O_3$, 245.1172). The ^1H and ^{13}C NMR spectra displayed characteristic resonances for a substituted naphthyl ring [δ_H 6.60 (H-3, s), 7.31 (H-5, s), 6.77 (H-9, s); δ_C 118.5 (C-1), 158.9 (C-2), 106.3 (C-3), 138.2 (C-4), 117.9 (C-5), 135.4 (C-6), 114.3 (C-7), 162.6 (C-8), 120.3 (C-9), 146.5 (C-10)], a methoxy group [δ_H 3.91 (2-OMe, s)] and three methyl groups [δ_H 2.76 (H_3-13, s), 2.80 (H_3-14, s), 2.48 (H_3-15, s)] (Table 1), which suggested the 12-norcadinane sesquiterpenoid skeleton of compound **1** (Yang and Shi, 2012). High similarities were revealed when comparing the ^1H and ^{13}C NMR spectroscopic data of compound **1** with the known compound commipholinone (Yang and Shi, 2012). Consequently, the HMBC correlations from H_3-15 to C-3 and C-5, from H-3 to C-1 and C-2, from H-5 to C-7 and C-6, and from 2-OMe to C-2 established the structure of compound **1** as 8-hydroxy-2-methoxynorcardina-2,4,6,8,10-pentaene-11-one (Fig. 2).

Commipholide A (**2**) was obtained as colorless oil (MeOH), and its molecular formula was determined as $C_{16}H_{16}O_4$ by the HRESIMS positive ion at *m/z* 273.1114 $[M + H]^+$ (calcd for $C_{16}H_{17}O_4$, 273.1121), with 9 indices of hydrogen deficiency. The 1D NMR spectroscopic data of **2** were mostly compatible with those of **1** (8 indices of hydrogen deficiency), except for the existence of an oxygenated quaternary carbon and a lactonic carbonyl carbon resonances [δ_C 74.5 (C-11), 178.9 (C-12)] (Table 1). Assignment of the 8,12-lactone moiety was accomplished by the HMBC correlations from H-9 to C-8, H_3-13 to C-12 and an extra index of hydrogen deficiency (Fig. 2). Besides, the position of the oxygenated quaternary carbon at C-11 was assigned by the HMBC correlations from H_3-13 to C-11, C-7, and C-12. Furthermore, in order to determine the absolute configuration of **2**, time dependent density functional theory (TDDFT) at the B3LYP/6–311++G (2d,p) level with IEFPCM in MeOH was used to calculate the ECD spectra of two enantiomers of **2** (Zhang, et al., 2021). The experimental ECD spectrum of **2** showed a negative Cotton effect (CE) at 260 nm ($\pi \rightarrow \pi^*$), a positive CE at 243 nm ($\pi \rightarrow \pi^*$), and a negative CE at 223 nm ($\pi \rightarrow \pi^*$), which coincided well with the calculated ECD spectrum of (11*S*)-**2** (Fig. 4). Thus, the structure of commipholide A (**2**) was determined as (11*S*)-11-hydroxy-2-methoxycardina-2,4,6,8,10-pentaene-8,12-olide.

Commiphone B (**3**) was obtained as colorless needles (MeOH), and its molecular formula was determined as $C_{15}H_{18}O_3$ by the HRESIMS positive ion at *m/z* 263.1275 $[M + H]^+$ (calcd for $C_{15}H_{19}O_3$, 263.1278). Compound **3** was a 12-norcadinane sesquiterpenoid possessing a 2,11-diketone moiety and a phenolic hydroxy group, which was suggested by its superimposable ^1H and ^{13}C NMR resonances in comparison with structurally similar compound **1** and commipholinone. Different functionality of **3** was suggested to be a methoxy group [δ_H 3.79 (8-OMe, s), δ_C 61.1 (8-OMe)] (Table 1), and its position was assigned at C-8 by the HMBC correlation from 8-OMe to C-8 (Fig. 2). Furthermore, the absolute configuration of **3** was identified as 4*S* by comparing the calculated and experimental ECD spectra (Fig. 5). Thus, the structure of commiphone B (**3**) was determined as (4*S*)-9-hydroxy-8-methoxynorcardina-1,7,9-trien-2,11-dione.

Commipholide B (**4**) was obtained as colorless oil (MeOH), and its molecular formula was determined as $C_{15}H_{18}O_3$ by the HRESIMS positive ion at *m/z* 247.1324 $[M + H]^+$ (calcd for $C_{15}H_{19}O_3$, 247.1329). The 1D and 2D NMR spectroscopic data of **4** were mostly compatible with those of known compounds myrrhanolides B and C (Shen, et al., 2009), except for the existence of an oxygenated methine [δ_H 5.00 (H-8, ddd, J = 13.2, 4.2, 1.8 Hz), δ_C 76.0 (C-8)] (Table 2). Its position was confirmed at C-8 by the ^1H–^1H COSY correlations between H-8/H-9/H-10/H_3-14 (Fig. 2). In addition, the NOESY correlations between H-8/H-9β/H_3-14, and H-10/H-9α indicated the β-orientations of H-8 and H_3-14 (Fig. 3). The α-orientation of H_3-15 was deduced from the NOESY correlations between H-4/H-5β, and H_3-15/H-3α. Furthermore, the absolute configuration of **4** was identified as 4*S*, 8*S*, and 10*S* by comparing the calculated and experimental ECD spectra (Fig. 6). Thus, the structure of commipholide B (**4**) was determined as (4*S*,8*S*,10*S*)-2-oxocadina-1(6),7(11)-dien-8,12-olide.

Commiphone C (**5**) was obtained as colorless oil (MeOH), and its molecular formula was determined as $C_{15}H_{16}O_3$ by the HRESIMS positive ion at *m/z* 245.1168 $[M + H]^+$ (calcd for $C_{15}H_{17}O_3$, 245.1172). The 1D NMR spectroscopic data of **5** were mostly compatible with those of myrrhone (Zhu, et al., 2003), except for the existence of an oxygenated methine [δ_H 5.25 (H-5, d, J = 2.2 Hz), δ_C 68.0 (C-5)] (Table 2). Its position was assigned at C-5 by the HMBC correlations from H_3-15 to C-5, from H-3 to C-5 and H-5 to C-6 (Fig. 2). Additionally, the α-orientations of H_3-15 and 5-OH were deduced from the NOESY correlations between H-3β/H-4/H-5, and H_3-15/H-3α (Fig. 3). Furthermore, the absolute configuration of **5** was identified as 4*S* and 5*S* by comparing the calculated and experimental ECD spectra (Fig. 7). Thus, the structure of commiphone C (**5**) was determined as (4*S*,5*S*)-5-hydroxyfuranocadina-1(6),9(10)-diene-2-one.

Commipholide C (**6**) was obtained as colorless oil (MeOH), and its molecular formula was determined as $C_{18}H_{24}O_6$ by the HRESIMS positive ion at *m/z* 359.1447 $[M + Na]^+$ (calcd for $C_{18}H_{24}O_6Na$, 359.1465). Compound **6** was a cadinane sesquiterpenoid possessing a 5α-acetoxy group and a 6,12-lactone moiety, which was suggested by its superimposable ^1H and ^{13}C NMR resonances in comparison with structurally similar known compound **3** in literature (Bhattacharya, et al., 1997). Different functionalities of **6** were suggested to be an α,β-unsaturated carbonyl moiety [δ_H 5.99 (H-9, s), δ_C 193.6 (C-8), 127.5 (C-9), 161.4

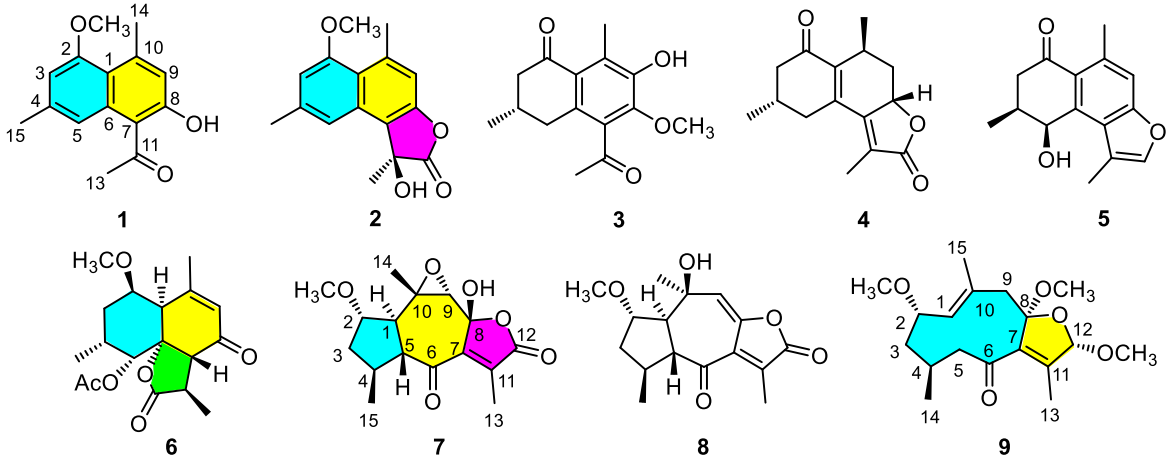

Fig. 1. Chemical structures of compounds **1**–**9**.

Table 1
^{1}H NMR and ^{13}C NMR spectroscopic data of compounds **1**–**3** (δ in ppm, and J in Hz, in $CDCl_3$).

NO.	**1**		**2**		**3**	
	δ_H	δ_C	δ_H	δ_C	δ_H	δ_C
1		118.5		132.1		137.7
2		158.9		159.0		198.9
3	6.60 (1H, s)	106.3	6.61 (1H, s)	107.0	2.67 (1H, ddd, J = 16.4, 3.8, 2.2 Hz) 2.25 (1H, dd, J = 16.4, 12.3 Hz)	48.4
4		138.2		138.6	2.17 (1H, m)	30.0
5	7.31 (1H, s)	117.9	7.43 (1H, s)	114.7	2.91 (1H, ddd, J = 16.3, 3.7, 2.2 Hz) 2.59 (1H, dd, J = 16.3, 10.8 Hz)	37.3
6		135.4		141.0		140.3
7		114.3		117.9		124.1
8		162.6		150.5		152.1
9	6.77 (1H, s)	120.3	6.95 (1H, s)	112.6		145.2
10		146.5		121.3		125.5
11		204.3		74.5		204.4
12				178.9		
13	2.76 (3H, s)	32.1	1.88 (3H, s)	22.3	2.60 (3H, s)	32.8
14	2.80 (3H, s)	26.3	2.88 (3H, s)	26.1	2.58 (3H, s)	21.4
15	2.48 (3H, s)	22.6	2.49 (3H, s)	25.2	1.10 (3H, d, J = 6.5 Hz)	15.0
2-OMe	3.91 (3H, s)	55.4	3.92 (3H, s)	55.3	3.79 (3H, s)	61.1
8-OH	12.91 (1H, s)					

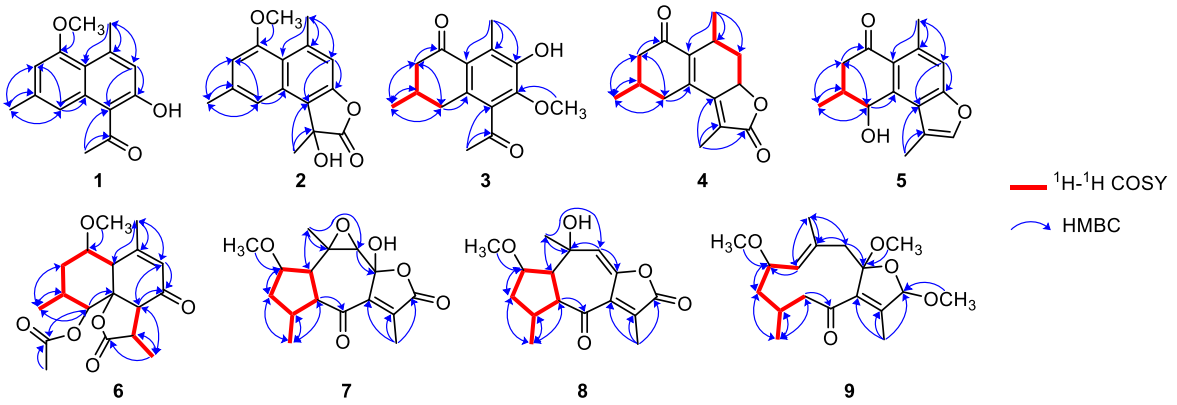

Fig. 2. Key ^{1}H–^{1}H COSY and HMBC correlations of compounds **1**–**9**.

Table 2
^{1}H NMR and ^{13}C NMR spectroscopic data of compounds **4**–**6** (δ in ppm, and J in Hz, in $CDCl_3$).

NO.	**4**		**5**		**6**	
	δ_H	δ_C	δ_H	δ_C	δ_H	δ_C
1		141.5		139.9	2.77 (1H, d, J = 11.4 Hz)	44.5
2		198.1		199.6	3.72 (1H, ddd, J = 11.4, 10.2, 6.0 Hz)	74.2
3	2.57 (1H, m) α 2.28 (1H, m) β	45.9	2.86 (1H, dd, J = 16.6, 13.4 Hz) α 2.52 (1H, dd, J = 16.6, 4.2 Hz) β	41.9	2.06 (1H, ddd, J = 16.8, 6.0, 5.4 Hz) β 1.76 (1H, ddd, J = 16.8, 10.2, 6.0 Hz) α	30.8
4	2.37 (1H, m)	29.1	2.43 (1H, m)	34.1	2.18 (1H, m)	31.9
5	3.08 (1H, m) β 2.37 (1H, m) α	34.7	5.25 (1H, d, J = 2.2 Hz)	68.0	4.82 (1H, d, J = 4.2 Hz)	73.6
6		141.0		138.9		85.1
7		154.9		124.8	2.90 (1H, d, J = 12.0 Hz)	51.4
8	5.00 (1H, ddd, J = 13.2, 4.2, 1.8 Hz)	76.0		157.9		193.6
9	2.28 (1H, m) β 1.66 (1H, m) α	35.7	7.30 (1H, s)	115.5	5.99 (1H, s)	127.5
10	3.23 (1H, m)	27.8		125.6		161.4
11		125.2		116.2	3.16 (1H, dq, J = 12.0, 8.4 Hz)	37.3
12		174.4	7.42 (1H, d, J = 1.4 Hz)	143.2		176.4
13	2.16 (3H, d, J = 1.8 Hz)	11.4	2.48 (3H, d, J = 1.5 Hz)	10.4	1.13 (3H, d, J = 7.3 Hz)	11.9
14	1.12 (3H, d, J = 6.4 Hz)	20.5	1.27 (3H, d, J = 6.8 Hz)	17.7	2.12 (3H, s)	23.1
15	1.20 (3H, d, J = 7.2 Hz)	19.7	2.73 (3H, s)	24.3	1.17 (3H, d, J = 7.5 Hz)	18.1
2-OMe					3.37 (3H, s)	55.5
5-OAc					2.13 (3H, s)	170.0 21.3

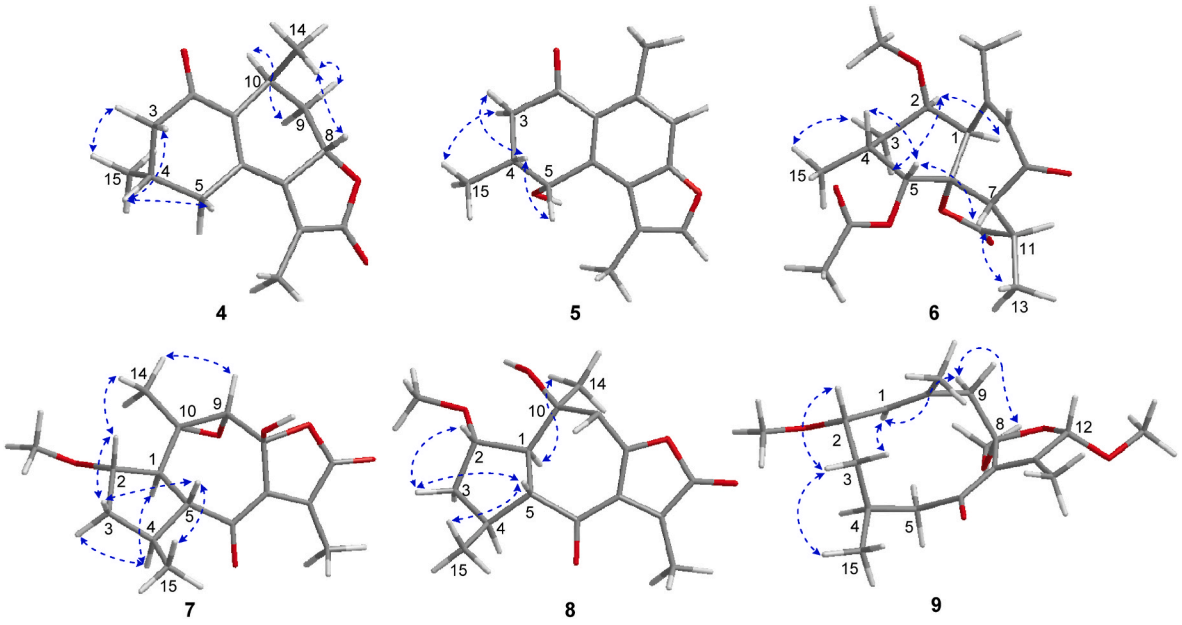

Fig. 3. Key NOESY correlations of compounds **4**–**9**.

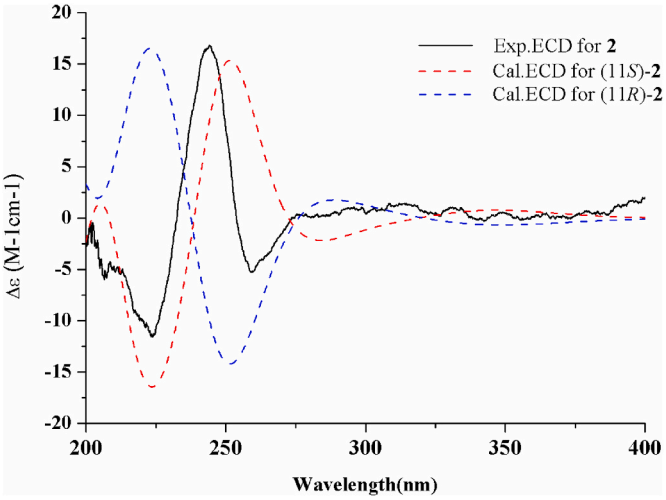

Fig. 4. Experimental and calculated ECD spectra of compound **2** (red and blue calculated at the B3LYP/6–311++G (2d,p)//B3LYP/6-31+G (d,p) level in MeOH; black, experimental in MeOH). (For interpretation of the references to color in this figure legend, the reader is referred to the Web version of this article.)

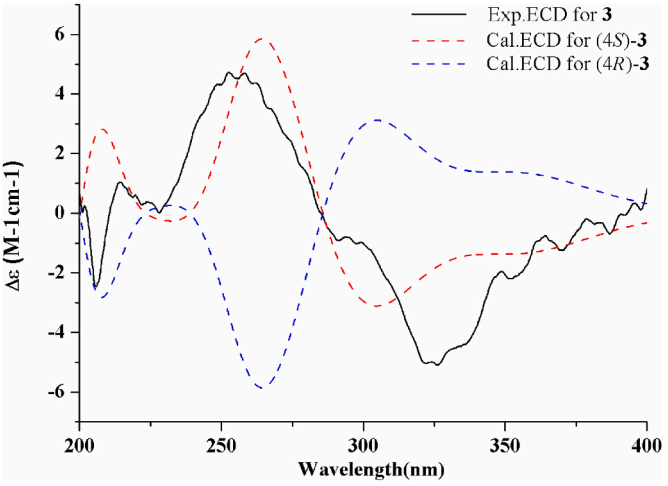

Fig. 5. Experimental and calculated ECD spectra of compound **3** (red and blue calculated at the B3LYP/6–311++G (2d,p)//B3LYP/6-31+G (d,p) level in MeOH; black, experimental in MeOH). (For interpretation of the references to color in this figure legend, the reader is referred to the Web version of this article.)

(C-10)], and a methoxy group [δ_H 3.37 (2-OMe, s), δ_C 55.5 (2-OMe)] (Table 2). The α,β-unsaturated carbonyl moiety was assigned as 9, 10-en-8-one by the HMBC correlations from H_3-14 to C-9, C-10, from H-9 to C-8, and from H-7 to C-8 (Fig. 2). The assignment of the methoxy group at C-2 was accomplished by the HMBC correlation from 2-OMe to C-2. In addition, the NOESY correlations between H-1/H-2/H-3α indicated the α-orientation of H-1, and the β-orientation of 2-OMe (Fig. 3). The NOESY correlations between H-4/H-5/H-7/H_3-13 indicated the β-orientations of H-7 and H_3-13, and the α-orientations of H_3-15 and 5-OAc. Furthermore, the absolute configuration of **6** was identified as 1*R*, 2*R*, 4*R*, 5*R*, 6*R*, 7*R* and 11*R* by comparing the calculated and experimental ECD spectra (Fig. 8). Thus, the structure of commipholide C (**6**) was determined as (1*R*,2*R*,4*R*,5*R*,6*R*,7*R*,11*R*)-5-acetoxy-2-methoxy-8-oxocadina-9-en-6,12-olide.

Commipholide D (**7**) was obtained as colorless jelly (MeOH), and its molecular formula was determined as $C_{16}H_{20}O_6$ by the HRESIMS positive ion at *m/z* 309.1329 $[M + H]^+$ (calcd for $C_{16}H_{21}O_6$, 309.1333). The ^{1}H NMR spectrum displayed characteristic resonances for three methyls [δ_H 1.00 (3H, d, J = 6.4 Hz), 1.46 (3H, s), 2.25 (3H, s)], and a methoxy group [δ_H 3.31 (3H, s)] (Table 3). Comprehensive analysis of the ^{13}C NMR and HSQC spectroscopic data suggested the presence of a keto-carbonyl group (δ_C 194.9), a lactonic carbonyl group (δ_C 169.9), a substituted vinyl group (δ_C 147.0 and 138.7), a hemiacetal group (δ_C 101.0), an oxygenated methine (δ_C 83.9), and an epoxy group (δ_C 66.6 and 64.7) (Table 3). Through a close comparison with the known compound 5β-10α-hydroxy-2α-methoxy-6-oxoguaia-7 (11),8-dien-8,12-olide (Shen, et al., 2008), compound **7** was suggested to be a guaiane sesquiterpenoid possessing a 2α-methoxy group, a 6-carbonyl group and a 8,12-lactone moiety. Other functionalities were suggested to be a 9, 10-epoxy group [δ_H 3.47 (H-9, s), δ_C 66.6 (C-9), 64.7 (C-10)] and a 8-hemiacetal group (δ_C 101.0) (Table 3), which were indicated by the HMBC correlations from H_3-14 to C-9, C-10, and from H-9 to C-8 (Fig. 2).

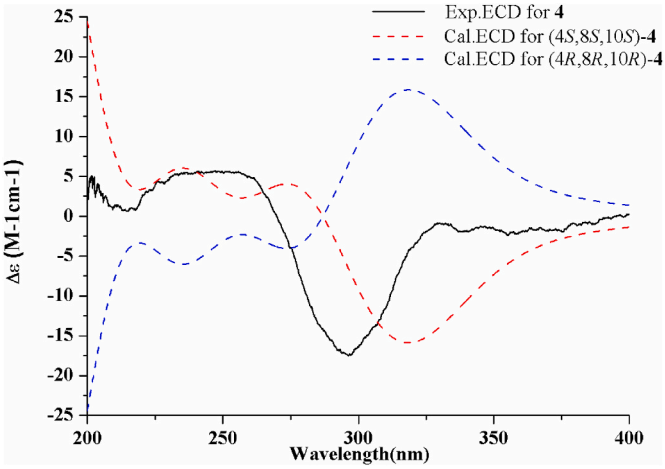

Fig. 6. Experimental and calculated ECD spectra of compound **4** (red and blue calculated at the B3LYP/6–311++G (2d,p)//B3LYP/6-31+G (d,p) level in MeOH; black, experimental in MeOH). (For interpretation of the references to color in this figure legend, the reader is referred to the Web version of this article.)

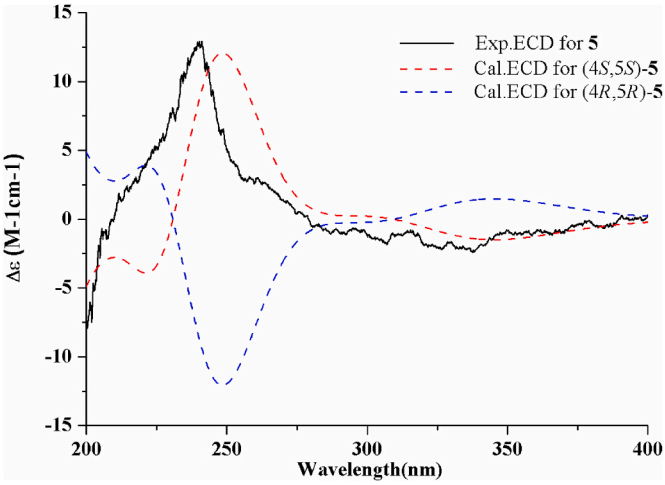

Fig. 7. Experimental and calculated ECD spectra of compound **5** (red and blue calculated at the B3LYP/6–311++G (2d,p)//B3LYP/6-31+G (d,p) level in MeOH; black, experimental in MeOH). (For interpretation of the references to color in this figure legend, the reader is referred to the Web version of this article.)

Moreover, the NOESY correlations between H-1/H-4/H-3α indicated the α-orientation of H-1, and the β-orientation of H_3-15 (Fig. 3). The NOESY correlations between H-2/H-3β/H-5, and H-2/H_3-14/H-9 indicated the β-orientations of H-5, H-9 and H_3-14, and the α-orientation of 2-OMe. However, the assignment of the orientation of 8-OH was a challenge due to the absence of associated NOESY correlations. Taking the biosynthetic pathways of guaiane sesquiterpenoid into consideration, TDDFT at the B3LYP/6–311++G (2d,p) level was used to calculate the ECD spectra of two possible candidates (1*S*,2*S*,4*S*,5*R*,8*R*,9*S*,10*S*)-**7**, and (1*S*,2*S*,4*S*,5*R*,8*S*,9*S*,10*S*)-**7**. As shown in Fig. 9, the experimental ECD spectrum of **7** showed a positive CE at 267 nm ($\pi \rightarrow \pi^*$), and a negative CE at 233 nm ($\pi \rightarrow \pi^*$), which coincided well with the calculated ECD spectrum of (1*S*,2*S*,4*S*,5*R*,8*R*,9*S*,10*S*)-**7**. Thus, the structure of commipholide D (**7**) was determined as (1*S*,2*S*,4*S*,5*R*,8*R*,9*S*,10*S*)-9,10-epoxy-8-hydroxy-2-methoxy-6-oxoguaia-7(11)-en-8,12-olide.

Commipholide E (**8**) was obtained as colorless needles (MeOH), and its molecular formula was determined as $C_{16}H_{20}O_5$ by the HRESIMS positive ion at *m/z* 293.1421 $[M + H]^+$ (calcd for $C_{16}H_{21}O_5$, 293.1389).

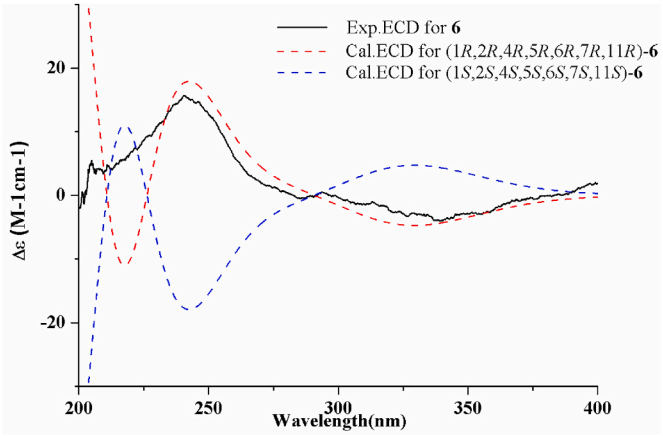

Fig. 8. Experimental and calculated ECD spectra of compound **6** (red and blue calculated at the B3LYP/6–311++G (2d,p)//B3LYP/6-31+G (d,p) level in MeOH; black, experimental in MeOH). (For interpretation of the references to color in this figure legend, the reader is referred to the Web version of this article.)

The ^{1}H and ^{13}C NMR spectroscopic data between compounds **8** and 5β-10α-hydroxy-2α-methoxy-6-oxoguaia-7 (11),8-dien-8,12-olide were superimposable but slight differences were observed (Table 3) (Shen, et al., 2008). Detailed analysis of 2D NMR data of **8** indicated the same planar structure compared to 5β-10α-hydroxy-2α-methoxy-6-oxoguaia-7 (11), 8-dien-8,12-olide. In the NOESY spectrum, a key correlation was observed between H-1/H_3-14 but not of H-5/H_3-14, indicating that H_3-14 is α-oriented (Fig. 3). Additionally, the absolute configuration of **8** was identified as 1*S*, 2*S*, 4*S*, 5*R*, and 10*R* by comparing the calculated and experimental ECD spectra (Fig. 10). Thus, the structure of commipholide E (**8**) was determined as (1*S*,2*S*,4*S*,5*R*,10*R*)-10-hydroxy-2-methoxy-6-oxoguai-7(11),8-dien-8,12-olide.

Commiphone D (**9**) was obtained as faint yellow oil (MeOH), and its molecular formula was determined as $C_{18}H_{28}O_5$ by the HRESIMS positive ion at *m/z* 325.2005 $[M + H]^+$ (calcd for $C_{18}H_{29}O_5$, 325.2009). Comprehensive analysis of the ^{1}H NMR, ^{13}C NMR and HSQC spectroscopic data of **9** suggested the presence of three methyls [δ_H 1.05 (3H, d, $J = 7.2$ Hz), 1.88 (3H, br s), 1.98 (3H, s)], three methoxy groups [δ_H 3.19 (3H, s), 3.20 (3H, s), 3.52 (3H, s)], an oxygenated methine [δ_H 4.01 (1H, td, $J = 9.4$, 2.8 Hz), δ_C 74.3], two olefinic bonds [(δ_H 4.93 (1H, d, $J = 9.0$ Hz), δ_C 132.2, 136.2, 136.3, 149.4], two hemiacetal groups [δ_H 5.21 (1H, s), δ_C 106.6, 115.7], and a keto-carbonyl group (δ_C 199.2) (Table 3). Through a close comparison with the known compound 8α-hydroxy-2α-methoxy-6-oxogermacra-1(10),7(11)-dien-8,12-olide (Yang and Shi, 2012; Shen et al., 2008), compound **9** was suggested to be a germacrane sesquiterpenoid possessing a 2α-methoxy group and a 6-carbonyl group. The major difference between **9** and the known compound was the absence of a lactonic carbonyl carbon resonance, which was replaced by a dioxygenated carbon resonance (δ_C 106.6) in **9**. Subsequently, its position was assigned at C-12 by the HMBC correlations from H_3-13 to C-7, C-11, C-12 (Fig. 2). Other functionalities were suggested to be 8-OMe and 12-OMe groups, which were indicated by the HMBC correlations from 8-OMe to C-8, and from 12-OMe to C-12. In addition, the NOESY correlations between H-1/H-3α/H-9α/8-OMe indicated the α-orientations of H-1 and 8-OMe (Fig. 3). The NOESY correlations between H-2/H-3β/H_3-15 indicated the β-orientation of H_3-15, and the α-orientation of 2-OMe. The determination of the orientation of 12-OMe was a challenge due to the absence of associated NOESY correlations. Hence, ^{13}C NMR chemical shift calculations at the mPW1PW91/6-311G+(d,p) level based on the gauge-independent atomic orbital (GIAO) were performed for the two epimers [(2*S**,4*S**,8*R**,12*S**)-**9** and (2*S**,4*S**,8*R**,12*R**)-**9**]. As a result, a higher correlation coefficient (R^2) value of 0.9982 for (2*S**,4*S**,8*R**,12*S**)-**9**, along with the parameters of DP4+

Table 3
^{1}H NMR and ^{13}C NMR spectroscopic data of compounds **7**–**9** (δ in ppm, and J in Hz, in $CDCl_3$).

NO.	**7**		**8**		**9**	
	δ_H	δ_C	δ_H	δ_C	δ_H	δ_C
1	2.20 (1H, dd, J = 12.6, 5.7 Hz)	53.5	2.17 (1H, dd, J = 10.2, 2.4 Hz)	56.9	4.93 (1H, d, J = 9.0 Hz)	132.2
2	3.93 (1H, ddd, J = 7.8, 5.7, 2.1 Hz)	83.9	3.97 (1H, dt, J = 5.9, 2.2, 2.2 Hz)	83.4	4.01 (1H, td, J = 9.4, 2.8 Hz)	74.3
3	2.01 (1H, ddd, J = 13.8, 7.6, 2.1 Hz) α	37.5	2.02 (1H, dd, J = 13.8, 6.0 Hz) α	38.9	1.95 (1H, m) α	36.3
	1.38 (1H, m) β		1.34 (1H, ddd, J = 13.8, 12.0, 6.0 Hz) β		1.62 (1H, ddd, J = 13.8, 5.1, 2.9 Hz) β	
4	2.52 (1H, m)	32.1	2.73 (1H, m)	32.3	2.41 (1H, m)	25.4
5	2.64 (1H, dd, J = 12.6, 10.5 Hz)	55.5	2.78 (1H, t, J = 9.8 Hz)	59.5	2.78 (1H, dd, J = 17.5, 10.3 Hz) 2.15 (1H, dd, J = 17.5, 5.3 Hz)	45.7
6		194.9		194.6		199.2
7		147.0		146.1		136.2
8		101.0		139.6		115.7
9	3.47 (1H, s)	66.6	5.82 (1H, d, J = 0.8 Hz)	118.6	2.66 (1H, d, J = 12.7 Hz) β 2.35 (1H, d, J = 12.7 Hz) α	51.0
10	3.23 (1H, m)	64.7		71.5		136.3
11		138.7		138.1		149.4
12		169.9		169.1	5.21 (1H, s)	106.6
13	2.25 (3H, s)	10.9	2.31 (3H, d, J = 0.8 Hz)	11.0	1.98 (3H, s)	12.3
14	1.46 (3H, s)	22.9	1.60 (3H, s)	30.1	1.05 (3H, d, J = 7.2 Hz)	21.9
15	1.00 (3H, d, J = 6.4 Hz)	18.6	1.06 (3H, d, J = 6.3 Hz)	18.8	1.88 (3H, br s)	19.4
2-OMe	3.31 (3H, s)	57.0	3.28 (3H, s)	56.5	3.20 (3H, s)	55.5
8-OMe					3.19 (3H, s)	50.5
12-OMe					3.52 (3H, s)	56.7

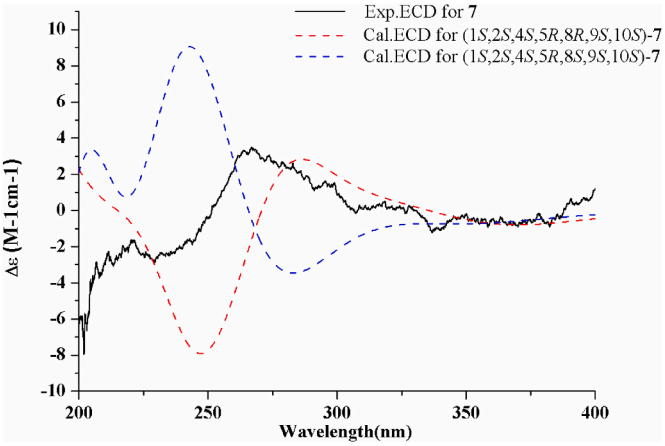

Fig. 9. Experimental and calculated ECD spectra of compound **7** (red and blue calculated at the B3LYP/6–311++G (2d,p)//B3LYP/6-31+G (d,p) level in MeOH; black, experimental in MeOH). (For interpretation of the references to color in this figure legend, the reader is referred to the Web version of this article.)

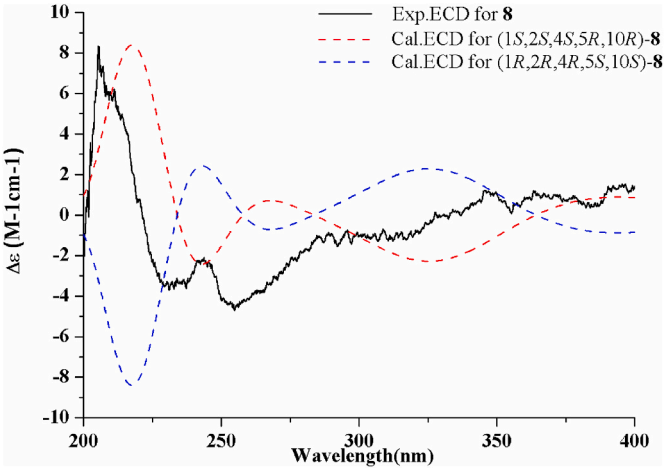

Fig. 10. Experimental and calculated ECD spectra of compound **8** (red and blue calculated at the B3LYP/6–311++G (2d,p)//B3LYP/6-31+G (d,p) level in MeOH; black, experimental in MeOH). (For interpretation of the references to color in this figure legend, the reader is referred to the Web version of this article.)

probability for two epimers [(2*S**,4*S**,8*R**,12*S**)-**9** 99.92% vs (2*S**,4*S**,8*R**,12*R**)-**9** 0.08%] confirmed the α-orientation of 12-OMe (Fig. S91 and Table S9−S10). Eventually, the absolute configuration of **9** was identified as 2*S*, 4*S*, 8*R*, and 12*S* by comparing the calculated and experimental ECD spectra (Fig. 11). Thus, the structure of commiphone D (**9**) was determined as (2*S*,4*S*,8*R*,12*S*)-8,12-epoxy-2,8,12-trimethoxygermacra-1,7-dien-6-one.

Myrrh has shown beneficial effects on various inflammation-related diseases such as ulcerative colitis, sepsis through inhibiting NO release and inflammatory factors *in vivo* and *in vitro* (Fatani et al., 2016; Kim et al., 2012). To identify whether these sesquiterpenoids isolated from the oleo-gum resin of *Commiphora myrrha* were the active components against inflammation, the sesquiterpenoids (**1**–**9**) were firstly evaluated for their inhibitory effects against LPS-induced NO production in RAW 264.7 mouse macrophages. The results showed that compared with the positive control hydrocortisone sodium succinate (HSS) (IC_{50} value = 74.47 ± 7.80 μM), commiphone A (**1**) and commipholide D (**7**) exhibited more potent inhibitory activity on NO generation with 24 h IC_{50} values of 18.6 ± 2.0 and 37.5 ± 1.5 μM, respectively, while the other compounds did not affect NO release induced by LPS (data were not shown). Meanwhile, up to 50 μM of all tested compounds did not induce cytotoxicity on the RAW264.7 cells (Figure S90). In addition, several inflammatory cytokines were measured in the RAW264.7 cells after co-treatment of different doses of **1** or **7** with LPS. As shown in Fig. 12, **1** and **7** significantly decreased the up-regulation of IL-1β and IL-6 mRNA expression induced by LPS. Meanwhile, **1** displayed stronger effects on the down-regulation of TNF-α expression compared with the positive control (40 μM HSS). Together, **1** and **7** exhibited potent NO production inhibitory activity caused by LPS in the mouse macrophages through reducing the expression of IL-1β, IL-6 and TNF-α.

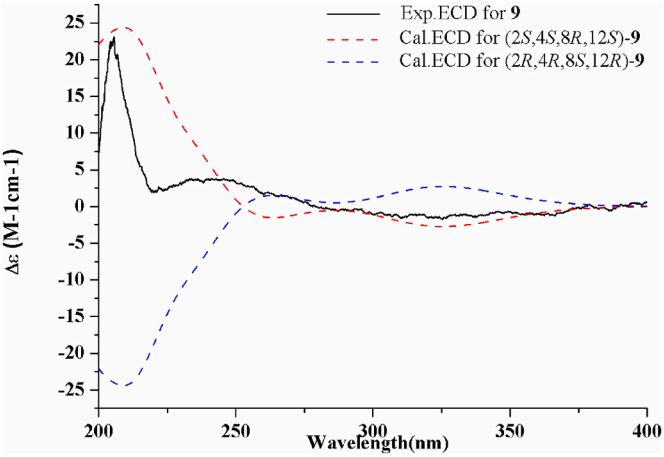

Fig. 11. Experimental and calculated ECD spectra of compound **9** (red and blue calculated at the B3LYP/6–311++G (2d,p)//B3LYP/6-31+G (d,p) level in MeOH; black, experimental in MeOH). (For interpretation of the references to color in this figure legend, the reader is referred to the Web version of this article.)

3. Conclusions

In summary, nine previously undescribed sesquiterpenoids were isolated from oleo-gum resin of *Commiphora myrrha*. These structures were determined through detailed analysis of spectroscopic data, and the comparison of calculated and experimental ECD spectra. Compounds **1**–**9** were undescribed sesquiterpenoids with different skeletons, which showcase the structural diversity of isolates obtained from the genus *Commiphora*. In addition, compounds **1** and **7** exhibited potent NO production inhibitory activity in LPS-treated RAW264.7 cells by reducing the expression of IL-1β, IL-6 and TNF-α.

4. Experimental

4.1. General experimental procedures

The UV spectra were obtained with a Shimadzu UV 2201 spectrophotometer. The ECD spectra were measured on a JASCO J-1500 spectropolarimeter in a 10 mm cell. The NMR spectra were recorded on Bruker AV-600 spectrometer or Bruker AV-500 with the measuring deuterated solvent as the internal reference. HRESIMS was conducted using a Waters ACQUITY SYNAPT™ G2 high-definition mass spectrometer or a Q-Exactive Hybrid Quadrupole Qrbitrap mass spectrometer. For preparative HPLC, a Waters 515 HPLC pump, equipped with a Shodex RI-101 Differential Refractometer detector and a JASCO UV-970 intelligent UV/VIS detector, was used. RP-HPLC separations were also conducted using a Shimadzu LC-6AD liquid chromatograph with an SPD-20 A UV detector equipped with a YMC Pack ODS-A column (250 × 20 mm, 120 Å, 5 μm). Silica gel GF_{254} (Qingdao Marine Chemical Factory, Shandong, P. R. China) was used for TLC. Column chromatography (CC) was performed on Silica gel (Qingdao Marine Chemical Factory), Octadesylsilanized (ODS) silica gel (Merck Chemical Company Ltd., Darmstadt, Germany), and Sephadex LH-20 (Amersham Pharmacia Biotech AB, Uppsala, Sweden). All reagents were of analytical grade (Concord Technology Co. Ltd., Tianjin, P. R. China).

4.2. Plant material

The oleo-gum resin of *Commiphora myrrha* (Nees) Engl. originated in Ethiopia, was furnished by Tianjin Tongrentang Group Co., Ltd. The resin was authenticated by Professor Lin Ma (Tianjin University of Traditional Chinese Medicine). The voucher specimen (accession number: 1038Q1512006) was deposited in the School of Chinese Materia Medica, Tianjin University of Traditional Chinese Medicine, P. R. China.

4.3. Extraction and isolation

The oleo-gum resin of *C. myrrha*. (3.0 kg) was powdered and extracted with CH_2Cl_2, then the extract was rotary evaporated to yield a residue (840 g). The residue was separated by silica gel CC, and eluted with a gradient of PE-EtOAc-MeOH (100:1:0, 50:1:0, 25:1:0, 10:1:0, 5:1:0, 3:1:0, 1:1:0, 0:1:0, 0:0:1) to afford six fractions (A-F).

Fraction B (152.9 g) was subjected to silica gel CC, and eluted with CH_2Cl_2–MeOH (250:1) to afford ten subfractions B-1 to B-10. Subfraction B-1 (7.9 g) was further subjected to Sephadex LH-20 CC with CH_2Cl_2–MeOH (1:1), and then separated by preparative-HPLC with hexane-EtOAc (9:1) to afford compound **2** (8.3 mg, t_R = 18.0 min). Subfraction B-2 (16.2 g) was subjected to ODS silica gel CC and eluted with a gradient of MeOH–H_2O to afford subfractions B-2-1 to B-2-3. Then, subfraction B-2-1 (1.2 g) was subjected to Sephadex LH-20 CC with CH_2Cl_2–MeOH (1:1), and then separated by preparative-HPLC with MeOH–H_2O (50:50) to afford compound **7** (1.8 mg, t_R = 36.3 min), and compound **9** (5.7 mg, t_R = 42.6 min). The subfraction B-2-2 (1.0 g) was subjected to Sephadex LH-20 CC with CH_2Cl_2–MeOH (1:1), and then separated by preparative-HPLC with MeOH–H_2O (50:50) to afford compound **5** (2.4 mg, t_R = 33.3 min). Subfraction B-3 (5.2 g) was subjected to ODS silica gel CC and eluted with a gradient of MeOH–H_2O to afford subfractions B-3-1 to B-3-5. Subfraction B-3-4 (1.1 g) was subjected to preparative-HPLC with MeOH–H_2O (60:40) to afford compound **8** (2.7 mg, t_R = 24.0 min). Subfraction B-3-5 (1.1 g) was subjected to preparative-HPLC with MeOH–H_2O (80:20) to afford compound **6** (2.1 mg, t_R = 34.8 min), and compound **4** (1.3 mg, t_R = 45.2 min). Subfraction B-5 (40.6 g) was subjected to ODS silica gel CC and eluted with a gradient of MeOH–H_2O to afford subfractions B-5-1 to B-5-6. Then, subfraction B-5-2 (771 mg) was subjected to Sephadex LH-20 CC with CH_2Cl_2–MeOH (1:1), and then separated by preparative-HPLC with MeOH–H_2O (60:40) to afford compound **1** (1.7 mg, t_R = 32.9 min). Similarly, subfraction B-5-3 (220 mg) was subjected to Sephadex LH-20 CC with CH_2Cl_2–MeOH (1:1), and then separated by preparative-HPLC with MeOH–H_2O (65:35) to afford compound **3** (1.8 mg, t_R = 20.3 min).

Commiphone A (1): pale yellow needles; UV (MeOH) λ_{max} (log ε) 203

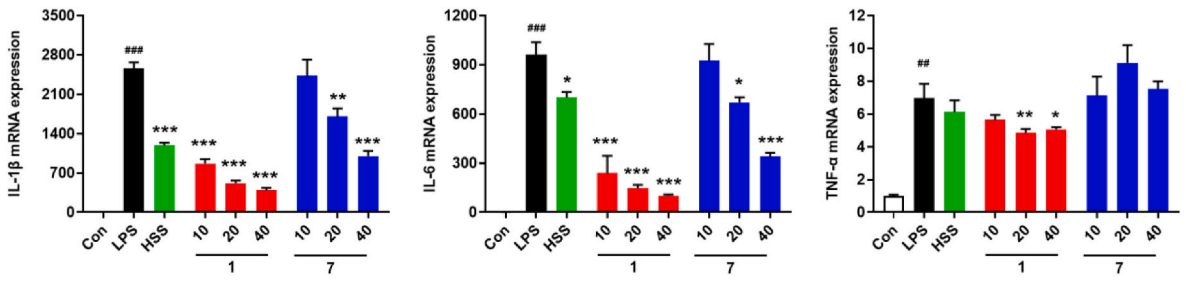

Fig. 12. Effects of **1** and **7** on the mRNA expression of IL-1β, IL-6 and TNF-α in the LPS-stimulated RAW264.7 cells treated with compounds **1** and **7** (10, 20 and 40 μM) or HSS (40 μM), respectively. Mean ± SD, n = 3. $^{*}P < 0.05$, $^{**}P < 0.01$, $^{***}P < 0.001$, *vs.* LPS-treated group; $^{\#\#}P < 0.01$, $^{\#\#\#}P < 0.001$, *vs.* Control group.

(3.89), 228 (3.92) nm; IR (KBr) ν_{max} 3361, 2921, 2849, 1649, 1609, 1456, 1355, 1263, 1175, 1072, 1026, 799 cm^{-1}; ^1H and ^{13}C NMR spectroscopic data, see Table 1; HRESIMS *m/z* 245.1167 $[M + H]^+$ (calcd for $C_{15}H_{17}O_3$, 245.1172).

Commipholide A ***(2)****:* colorless oil; UV (MeOH) λ_{max} (log ε) 203 (3.94), 228 (3.97) nm; ECD (*c* 1.2 × 10^{-4} M, MeOH) λ_{max} ($\Delta\varepsilon$) 223 (−11.57), 243 (+16.47), 260 (−5.28) nm; IR (KBr) ν_{max} 3376, 2973, 2933, 2855, 1812, 1628, 1590, 1455, 1346, 1259, 1183, 1156, 1055, 1015, 951, 833 cm^{-1}; ^1H and ^{13}C NMR spectroscopic data, see Table 1; HRESIMS *m/z* 273.1114 $[M + H]^+$ (calcd for $C_{16}H_{17}O_4$, 273.1121).

Commiphone B ***(3)****:* colorless needles; UV (MeOH) λ_{max} (log ε) 203 (3.88), 247 (3.67), 274 (3.64) nm; ECD (*c* 1.3 × 10^{-4} M, MeOH) λ_{max} ($\Delta\varepsilon$) 222 (+0.27), 253 (+4.72), 326 (−5.08) nm; IR (KBr) ν_{max} 3325, 2954, 2929, 2872, 1697, 1671, 1567, 1456, 1410, 1355, 1315, 1301, 1205, 1186, 1163, 1040, 933, 845 cm^{-1}; ^1H and ^{13}C NMR spectroscopic data, see Table 1; HRESIMS *m/z* 263.1275 $[M + H]^+$ (calcd for $C_{15}H_{19}O_3$, 263.1278).

Commipholide B ***(4)****:* colorless oil; UV (MeOH) λ_{max} (log ε) 202 (3.41), 294 (3.47) nm; ECD (*c* 2.0 × 10^{-4} M, MeOH) λ_{max} ($\Delta\varepsilon$) 215 (+0.63), 296 (−17.54) nm; IR (KBr) ν_{max} 2957, 2919, 2849, 1754, 1668, 1645, 1468, 1280, 1259, 1116, 1046, 799 cm^{-1}; ^1H and ^{13}C NMR spectroscopic data, see Table 2; HRESIMS *m/z* 247.1324 $[M + H]^+$ (calcd for $C_{15}H_{19}O_3$, 247.1329).

Commiphone C ***(5)****:* colorless needles; UV (MeOH) λ_{max} (log ε) 203 (3.60), 240 (3.89) nm; ECD (*c* 2.4 × 10^{-4} M, MeOH) λ_{max} ($\Delta\varepsilon$) 241 (+12.93) nm; IR (KBr) ν_{max} 3388, 2961, 2928, 2854, 1737, 1672, 1590, 1453, 1343, 1312, 1256, 1160, 1100, 1059, 1040, 940, 857, 793 cm^{-1}; ^1H and ^{13}C NMR spectroscopic data, see Table 2; HRESIMS *m/z* 245.1168 $[M + H]^+$ (calcd for $C_{15}H_{17}O_3$, 245.1172).

Commipholide C ***(6)****:* colorless oil; UV (MeOH) λ_{max} (log ε) 203 (3.72), 235 (3.43) nm; ECD (*c* 1.8 × 10^{-4} M, MeOH) λ_{max} ($\Delta\varepsilon$) 241 (+15.69), 340 (−4.01) nm; IR (KBr) ν_{max} 3362, 2926, 2851, 1783, 1736, 1671, 1619, 1457, 1375, 1258, 1233, 1182, 1088, 1028, 797 cm^{-1}; ^1H and ^{13}C NMR spectroscopic data, see Table 2; HRESIMS *m/z* 359.1447 $[M + Na]^+$ (calcd for $C_{18}H_{24}O_6Na$, 359.1465).

Commipholide D ***(7)****:* colorless jelly; UV (MeOH) λ_{max} (log ε) 202 (3.47) nm; ECD (*c* 1.9 × 10^{-4} M, MeOH) λ_{max} ($\Delta\varepsilon$) 233 (−2.50), 267 (+3.43) nm; IR (KBr) ν_{max} 3351, 2927, 2853, 1773, 1699, 1653, 1453, 1383, 1218, 1081, 1018, 937 cm^{-1}; ^1H and ^{13}C NMR spectroscopic data, see Table 3; HRESIMS *m/z* 309.1329 $[M + H]^+$ (calcd for $C_{16}H_{21}O_6$, 309.1333).

Commipholide E ***(8)****:* colorless needles; UV (MeOH) λ_{max} (log ε) 203 (3.95) nm; ECD (*c* 1.1 × 10^{-4} M, MeOH) λ_{max} ($\Delta\varepsilon$) 205 (+8.33), 237 (−3.63), 243 (−2.19), 252 (−4.42) nm; IR (KBr) ν_{max} 3410, 2955, 2929, 1771, 1701, 1457, 1377, 1197, 1095, 1025, 948 cm^{-1}; ^1H and ^{13}C NMR spectroscopic data, see Table 3; HRESIMS *m/z* 293.1421 $[M + H]^+$ (calcd for $C_{16}H_{21}O_5$, 293.1389).

Commiphone D ***(9)****:* faint yellow oil; UV (MeOH) λ_{max} (log ε) 203 (4.49), 226 (4.30) nm; ECD (*c* 3.4 × 10^{-5} M, MeOH) λ_{max} ($\Delta\varepsilon$) 204 (+22.56), 223 (+2.11), 241 (+3.83) nm; IR (KBr) ν_{max} 2927, 2834, 1681, 1638, 1447, 1370, 1307, 1280, 1188, 1161, 1108, 1059, 1046, 976, 961, 906, 875, 706 cm^{-1}; ^1H and ^{13}C NMR spectroscopic data, see Table 3; HRESIMS *m/z* 325.2005 $[M + H]^+$ (calcd for $C_{18}H_{29}O_5$, 325.2009).

4.4. ECD and NMR calculations

The details of the quantum chemical ECD and NMR calculations for compounds **2**–**9** are provided in Supporting Information.

4.5. NO inhibitory assays and cell viability

The RAW 264.7 mouse macrophages were obtained from National Collection of Authenticated Cell Cultures, and were cultured in RPMI 1640 medium (Procell, Wuhan, China) with penicillin G sodium salt, streptomycin sulfate and 10% fetal bovine serum (FBS). The cells were seeded in 96-well plastic plates with 1 × 10^5 cells/well and allowed to adhere at 37 °C for 24 h in a humidified atmosphere containing 5% CO_2. Then, the medium was replaced with fresh medium containing LPS (1 μg/ml) together with different concentrations of compound **1**–**9** or HSS for 24 h. NO production was determined by measuring the accumulation of nitrite in the culture supernatant using a Griess reagent. The process was conducted according to the literature (Cao, et al., 2019). After transferring the required supernatant to another plate for the Griess assay, the cell viability was measured by the MTT assay based on previous studies (Sun, et al., 2016).

4.6. Determination of mRNA expression of IL-1β, IL-6 and TNF-α by qPCR

RAW 264.7 cells were seeded in 6-well plastic plates with 10 × 10^5 cells/well. After 24 h, the cells were treated with LPS (1 μg/ml) with or without different concentrations of compound **1** and **7** (10, 20, and 40 μM) or HSS (40 μM) for 24 h. After total RNA isolated from the RAW264.7 cells was converted to cDNA, and then qPCR was performed according to our previous published study (Zhao, et al., 2020). The primers of IL-1β, IL-6, TNF-α and GAPDH were listed in Table S13.

4.7. Statistical analysis

SPSS 19.0 software was used for statistical analysis of the data. Data are expressed as mean ± standard deviation (Mean ± SD). One-way analysis of variance (One-way ANOVA) was used for comparison between groups. $P < 0.05$ was used as statistically significant.

CRediT authorship contribution statement

Bingyang Zhang: Writing – original draft, Methodology, Conceptualization. **Wenhua Chao:** Formal analysis, Data curation. **Weiyun Di:** Validation, Data curation. **Shijie Cao:** Writing – original draft, Methodology, Conceptualization. **Paul Owusu Donkor:** Writing – review & editing. **Lining Wang:** Validation, Resources. **Feng Qiu:** Writing – review & editing, Validation, Funding acquisition, Conceptualization.

Declaration of competing interest

The authors declare the following financial interests/personal relationships which may be considered as potential competing interests: Feng Qiu reports financial support was provided by National Key Research and Development Program of China. If there are other authors, they declare that they have no known competing financial interests or personal relationships that could have appeared to influence the work reported in this paper.

Data availability

Data will be made available on request.

Acknowledgements

This research was supported financially by the National Key Research and Development Program of China (2019YFC1711000), and the "Killer" Products Cultivation Project of Xiqing District, Tianjin (xqssj- 202016).

Appendix A. Supplementary data

Supplementary data to this article can be found online at https://doi.org/10.1016/j.phytochem.2024.114031.

References

Abdul-Ghani, R.A., Loutfy, N., Hassan, A., 2009. Myrrh and trematodoses in Egypt: an overview of safety, efficacy and effectiveness profiles. Parasitol. Int. 58, 210–214. https://doi.org/10.1016/j.parint.2009.04.006.

Al-Romaiyan, A., Huang, G.C., Jones, P., Persaud, S., 2021. *Commiphora myrrha* stimulates insulin secretion from mouse and human islets of Langerhans. J. Ethnopharmacol. 264, 113075 https://doi.org/10.1016/j.jep.2020.113075.

Bao, S., Li, C., Li, H., Wang, J., Luan, J., Zhang, Y., Chen, L., Hu, Y., Chang, X., 2021. Myrrhterpenes A and B, anti-inflammatory cadinane sesquiterpenes from the resin of *Commiphora myrrha*. Phytochem. Lett. 44, 190–194. https://doi.org/10.1016/j.phytol.2021.06.024.

Bhattacharya, A.K., Jain, D.C., Sharma, R.P., Roy, R., Mcphail, A.T., 1997. Boron trifluoride-acetic anhydride catalysed rearrangement of dihydroarteannuin B. Tetrahedron 53, 14975–14990. https://doi.org/10.1016/S0040-4020(97)01049-1.

Cao, Y., Chen, J., Ren, G., Zhang, Y., Tan, X., Yang, L., 2019. Punicalagin prevents inflammation in LPS-induced RAW264.7 macrophages by inhibiting FoxO3a/autophagy signaling pathway. Nutrients 11, 2794. https://doi.org/10.3390/nu11112794.

Committee of the Chinese Pharmacopia, 2020. The Chinese Pharmacopia, vol. 1. China Medical Science Press, Beijing.

Demissew, S., 1993. A description of some essential oil bearing plants in Ethiopia and their indigenous uses. J. Essent. Oil Res. 5, 465–479. https://doi.org/10.1080/10412905.1993.9698266.

Fatani, A.J., Alrojayee, F.S., Parmar, M.Y., Abuohashish, H.M., Ahmed, M.M., Al-Rejaie, S.S., 2016. Myrrh attenuates oxidative and inflammatory processes in acetic acid-induced ulcerative colitis. Exp. Ther. Med. 12, 730–738. https://doi.org/10.3892/etm.2016.3398.

Khalil, N., Fikry, S., Salama, O., 2020. Bactericidal activity of Myrrh extracts and two dosage forms against standard bacterial strains and multidrug-resistant clinical isolates with GC/MS profiling. Amb. Express 10, 21. https://doi.org/10.1186/s13568-020-0958-3.

Kim, M.S., Bae, G.S., Park, K.C., Koo, B.S., Kim, B.J., Lee, H.J., Seo, S.W., Shin, Y.K., Jung, W.S., Cho, J.H., Kim, Y.C., Kim, T.H., Song, H.J., Park, S.J., 2012. Myrrh inhibits LPS-induced inflammatory response and protects from cecal ligation and puncture-induced sepsis. Evid. Based Complement Alternat. Med., 278718 https://doi.org/10.1155/2012/278718, 2012.

Shen, T., Li, G.H., Wang, X.N., Lou, H.X., 2012. The genus *commiphora*: a review of its traditional uses, phytochemistry and pharmacology. J. Ethnopharmacol. 142, 319–330. https://doi.org/10.1016/j.jep.2012.05.025.

Shen, T., Wan, W.Z., Wang, X.N., Sun, L.M., Yuan, H.Q., Wang, X.L., Ji, M., Lou, H.X., 2008. Sesquiterpenoids from the resinous exudates of *Commiphora opobalsamum* (Burseraceae). Helv. Chim. Acta 91, 881–886. https://doi.org/10.1002/hlca.200890092.

Shen, T., Wan, W.Z., Wang, X.N., Yuan, H.Q., Ji, M., Lou, H.X., 2009. A triterpenoid and sesquiterpenoids from the resinous exudates of *Commiphora myrrha*. Helv. Chim. Acta 92, 645–652. https://doi.org/10.1002/hlca.200800347.

Sun, C.P., Qiu, C.Y., Yuan, T., Nie, X.F., Sun, H.X., Zhang, Q., Li, H.X., Ding, L.Q., Zhao, F., Chen, L.X., Qiu, F., 2016. Antiproliferative and anti-inflammatory withanolides from *Physalis angulata*. J. Nat. Prod. 79, 1586–1597. https://doi.org/10.1021/acs.jnatprod.6b00094.

Sun, M., Hua, J., Liu, G., Huang, P., Liu, N., He, X., 2020. Myrrh induces the apoptosis and inhibits the proliferation and migration of gastric cancer cells through down-regulating cyclooxygenase-2 expression. Biosci. Rep. 40, BSR20192372 https://doi.org/10.1042/BSR20192372.

Wang, C.C., Liang, N.Y., Xia, H., Wang, R.Y., Zhang, Y.F., Huo, H.X., Zhao, Y.F., Song, Y.L., Zheng, J., Tu, P.F., Li, J., 2022. Cytotoxic sesquiterpenoid dimers from the resin of *Commiphora myrrha*. Engl. Phytochemistry 204, 113443. https://doi.org/10.1016/j.phytochem.2022.113443.

Yang, J.L., Shi, Y.P., 2012. Cycloartane-type triterpenoids and sesquiterpenoids from the resinous exudates of *Commiphora opobalsamum*. Phytochemistry 76, 124–132. https://doi.org/10.1016/j.phytochem.2012.01.004.

Yu, Y.F., Liu, Y.H., Chen, X.H., Zhi, D.J., Qi, F.M., Zhang, Z.P., Li, Y.Q., Zhang, Z.X., Fei, D.Q., 2020. Cadinane-type sesquiterpenes from the resinous exudates of *Commiphora myrrha* and their anti-alzheimer's disease bioactivities. Fitoterapia 142, 104536. https://doi.org/10.1016/j.fitote.2020.104536.

Zhang, B., Liu, D., Cao, S., Yao, T., Liu, G., Chen, L., Qiu, F., 2022. Anti-proliferative tirucallane triterpenoids from gum resin of *Boswellia sacra*. Bioorg. Chem. 129, 106155 https://doi.org/10.1016/j.bioorg.2022.106155.

Zhang, B., Liu, D., Ji, W., Otsuki, K., Higai, K., Zhao, F., Li, W., Koike, K., Qiu, F., 2021. Sacraoxides A-G, bioactive cembranoids from gum resin of *Boswellia sacra*. Front. Chem. 9, 649287 https://doi.org/10.3389/fchem.2021.649287.

Zhao, S.J., Kong, F.Q., Jie, J., Li, Q., Liu, H., Xu, A.D., Yang, Y.Q., Jiang, B., Wang, D.D., Zhou, Z.Q., Tang, P.Y., Chen, J., Wang, Q., Zhou, Z., Chen, Q., Yin, G.Y., Zhang, H.W., Fan, J., 2020. Macrophage MSR1 promotes BMSC osteogenic differentiation and M2-like polarization by activating PI3K/AKT/GSK3β/β-catenin pathway. Theranostics 10, 17–35. https://doi.org/10.7150/thno.36930.

Zhu, N., Sheng, S., Sang, S., Rosen, R.T., Ho, C.T., 2003. Isolation and characterization of several aromatic sesquiterpenes from *Commiphora myrrha*. Flavour Fragrance J. 18, 282–285. https://doi.org/10.1002/ffj.1193.